Nonlinear wave chaos: statistics of second harmonic fields

Min Zhou,[1,2] Edward Ott,[1,3] Thomas M. Antonsen, Jr.,[1,3] and Steven M. Anlage[1,2,3]
[1]*Department of Electrical and Computer Engineering, University of Maryland, College Park, Maryland 20742-3285, USA*
[2]*Center for Nanophysics and Advanced Materials, University of Maryland, College Park, Maryland 20742-4111, USA*
[3]*Department of Physics, University of Maryland, College Park, Maryland 20742-4111, USA*

(Received 5 June 2017; accepted 21 September 2017; published online 12 October 2017)

Concepts from the field of wave chaos have been shown to successfully predict the statistical properties of linear electromagnetic fields in electrically large enclosures. The Random Coupling Model (RCM) describes these properties by incorporating both universal features described by Random Matrix Theory and the system-specific features of particular system realizations. In an effort to extend this approach to the nonlinear domain, we add an active nonlinear frequency-doubling circuit to an otherwise linear wave chaotic system, and we measure the statistical properties of the resulting second harmonic fields. We develop an RCM-based model of this system as two linear chaotic cavities coupled by means of a nonlinear transfer function. The harmonic field strengths are predicted to be the product of two statistical quantities and the nonlinearity characteristics. Statistical results from measurement-based calculation, RCM-based simulation, and direct experimental measurements are compared and show good agreement over many decades of power. *Published by AIP Publishing.* https://doi.org/10.1063/1.4986499

The wave properties of systems that show chaos in the classical limit, and are large compared to the wavelength, are extensively studied in the field of "wave chaos." These systems are quite common in life, ranging from the small scale of atomic nuclei, to mesoscopic quantum systems like quantum dots, to macroscopic acoustic, microwave, optical systems, and even to ocean waves in the sea. The Random Coupling Model (RCM) is a well-established theory that describes the statistical wave scattering properties of these wave chaotic systems. A two-dimensional 1/4-bowtie microwave billiard is one example of a wave chaotic system that has been studied experimentally and numerically. Microwave experiments in these billiards have demonstrated the accuracy of the RCM. However, prior work has been confined to linear systems, and has not taken into account nonlinearity in the wave properties, which is potentially important. By adding an active circuit that generates second harmonics to the 1/4 bowtie-billiard, this work is the first step in trying to generalize the RCM to nonlinear systems, specifically by focusing on the second harmonic field statistics. An extended RCM model that includes the characteristics of the nonlinear element shows very good agreement with the experimental results.

I. INTRODUCTION

The scattering of short-wavelength waves in domains in which the corresponding rays are chaotic (known as wave chaos) has inspired research activities in many diverse contexts including quantum dots,[1,2] atomic nuclei,[3] optical cavities,[4] microwave cavities,[5–7] acoustic resonators,[8,9] and others. In this case, the response is extremely sensitive to the domain's configuration, the driving frequency, and ambient conditions such as temperature and pressure.[10] Numerical solution of the detailed response of a particular system is computationally intensive and does not necessarily provide much insight into other systems which are slightly different. This leads to the adoption of a statistical description.

It is hypothesized that the wave properties of classically chaotic billiard systems show universal statistical properties described by the Random Matrix Theory (RMT).[11–13] The statistics depend only on general symmetries, inlcuding the presence or absence of time-reversal invariance and spin-1/2 degree of freedom, and on the degree of loss. In the field of "wave chaos," Random Matrix Theory (RMT) has been shown to successfully describe many statistical properties of bounded wave-chaotic systems (e.g., enclosures such as electromagnetic cavities), including their eigenvalue spectra, eigenfunctions, scattering matrices, delay times, etc.[13–20] Wave systems also have system-specific features that modify the underlying universal fluctuations. The Random Coupling Model (RCM) accounts for those non-universal features such as the details of ports coupling waves into and out of the domain of the cavity, short orbits that exist between the ports, and specific persistent features of the enclosure in an ensemble of similar but different realizations of a system.[21–23] Experimentally, the system-specific features are captured by the impedance (reaction matrix)[24] averaged over an ensemble of realizations. By applying this technique to remove non-universal properties, the RMT statistical properties have been uncovered in experimental data on ray chaotic 1D quantum graphs,[25] 2D electromagnetic cavities (known as billiards),[26] and 3D cavities [e.g., reverberation chambers (RC)].[27]

Based on the success of the RCM, it is of interest to explore directions extending its generality. Along this line, theories have been developed for "mixed" systems which include both regular and chaotic ray dynamics,[28] and for networks of coupled cavities in which waves propagate from

one sub-system to another.[29,30] While such previous extensions have focused on linear systems, it is of great interest to see how nonlinearity would modify the RCM. The present paper is meant to serve as a first step towards a nonlinear generalization of the RCM by examining the statistics of nonlinearly generated harmonic signals.

Nonlinearity has arisen before in the study of wave chaos. For example, rouge waves can appear in wave chaotic scattering systems.[31,32] They appear in different physical contexts and are enhanced by nonlinear mechanisms.[33,34] In acoustics, Time-Reversed Nonlinear Elastic Wave Spectroscopy (TR/NEWS) is based on the nonlinear time reversal properties of a wave chaotic system.[35] TR/NEWS is proposed as a tool to detect micro-scale damage features (e.g., delaminations, microcracks or weak adhesive bonds) *via* their nonlinear acoustic signatures.[36,37] Applying this idea to electromagnetic waves,[38] the nonlinear electromagnetic time-reversal mirror shows promise for novel applications such as exclusive communication and wireless power transfer.[39,40] A theoretical study of stationary scattering from quantum graphs has been generalized to the nonlinear domain, where the nonlinearity creates multi-stability and hysteresis.[41] A wave-chaotic microwave cavity with a nonlinear circuit feedback loop demonstrated subwavelength position sensing for a perturber inside a cavity.[42] Furthermore, investigation of the electromagnetic field statistics created by nonlinear electronics inside a wave chaotic reverberation chamber has a number of applications, including electromagnetic immunity testing of digital electronics.[43,44]

In this work, an active nonlinear circuit is added to a ray-chaotic microwave billiard. The billiard, shown schematically in Fig. 1, has an area of $A = 0.115\ \mathrm{m}^2$, with a corresponding characteristic length of $A^{1/2} = 0.34$ m. For the microwave wavelengths used here (3 − 9 cm), the billiard is assumed to be large compared to the wavelength (electrically large enclosure) and is considered to be in the semiclassical

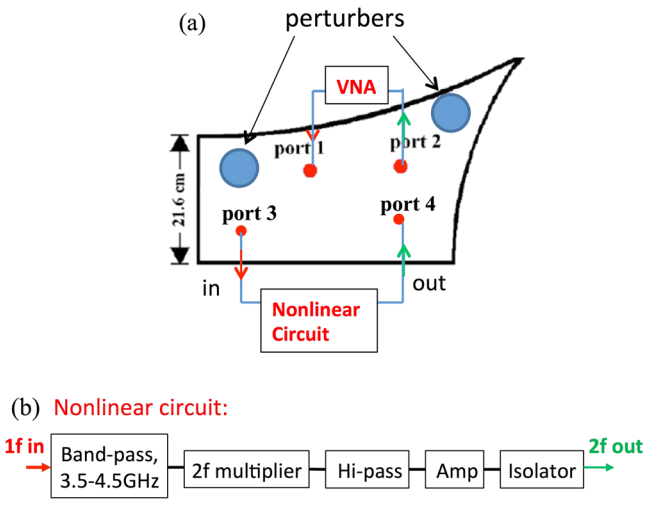

FIG. 1. Experimental setup: 1/4-bowtie cavity with an active nonlinear circuit. (a) The vector network analyzer (Model: Keysight PNA N5242A or E8364C) measures the absolute power of harmonics at port 2 relative to the input fundamental tone at port 1. (b) The active nonlinear circuit consists of two cascaded 3.5 GHz–4.5 GHz band pass filters (Mini-Circuit VBFZ-4000-S+), a frequency doubler (Mini-Circuit ZX9C-2–50-S+), two cascaded high pass filters (Mini-circuit VHF-6010+), a wide band power amplifier (HP83020A), and an isolator (FairviewMicrowave SFI 0418).

or short-wavelength limit. The cavity has a height of $d = 7.9$ mm. Thus, below a frequency $f_{max} = c/(2d) = 18.9$ GHz, it is a quasi-2D billiard in which the electric field is polarized in the short direction, and the magnetic field is in the 2D plane of the cavity. For frequencies $2f > 7$ GHz, the mode number is above ∼200 and it can be considered that the cavity is in the highly over-moded regime (where there are many cavity modes at and below the frequency of interest).[6] The cavity has internal loss, giving rise to a finite quality factor (Q) for the resonant modes of the closed system. We shall assume that a single Q describes the losses in a given range of frequency.[45] The nonlinear circuit accepts input at a particular frequency and generates and amplifies second harmonic output which is fed back into the billiard. We study the statistics of the second harmonic fields in the cavity for a fixed power at the input fundamental frequency.

II. BACKGROUND AND EXPERIMENTAL SETUP

In the case of a linear ray-chaotic cavity with N ports, the Random Coupling Model characterizes the fluctuations in the impedance $\overline{\overline{Z}}$ and scattering $\overline{\overline{S}}$ matrices. The scattering and impedance matrices are related by a simple bilinear transformation[46]

$$\overline{\overline{S}} = \overline{\overline{Z}}_0^{1/2}(\overline{\overline{Z}} + \overline{\overline{Z}}_0)^{-1}(\overline{\overline{Z}} - \overline{\overline{Z}}_0)\overline{\overline{Z}}_0^{-1/2}, \tag{1}$$

where $\overline{\overline{Z}}_0$ is a real diagonal matrix whose elements are the characteristic impedances of the waveguide (or transmission line) input channels at the driving ports. The statistical properties of the cavity impedance $\overline{\overline{Z}}_{cav}$ are described by a universally fluctuating impedance $\overline{\overline{\xi}}$ that is 'dressed' by system-specific properties captured by the ensemble average impedance $\overline{\overline{Z}}_{avg}$ as

$$\overline{\overline{Z}}_{cav} = i \cdot Im(\overline{\overline{Z}}_{avg}) + \left[Re(\overline{\overline{Z}}_{avg})\right]^{\frac{1}{2}} \cdot \overline{\overline{\xi}} \cdot \left[Re(\overline{\overline{Z}}_{avg})\right]^{\frac{1}{2}}, \tag{2}$$

where $\overline{\overline{Z}}_{avg}$ is an average of impedance over an ensemble of cavity realizations and(or) frequencies. $\overline{\overline{Z}}_{avg}$ contains the system specific features including the radiation impedance of the ports and short orbits that survive the ensemble averages.[21–23] The "radiation impedance" represents the impedance measured at the ports of the scattering enclosure in the case that the waves are allowed to enter the enclosure through the port but not return, as if they were absorbed in the enclosure or radiated to infinity. Experimentally, it can be measured with the empty bowtie billiard whose boundary is covered with perfect microwave absorbers. A "short orbit" is a ray trajectory that leaves a port and soon returns to it, or another port, instead of ergodically sampling the system. It is the result of the port-port interaction that introduces deterministic field components which can remain fixed throughout the ensemble.[23] $\overline{\overline{Z}}_{avg}$ can also be estimated if the radiation impedance of the ports and the cavity shape are known.[21]

By inverting Eq. (2) and subtracting the non-universal features from $\overline{\overline{Z}}_{cav}$ in each realization, one can uncover a statistically fluctuating quantity that should correspond to $\overline{\overline{\xi}}$. It has been hypothesized that all sufficiently complex wave chaotic systems have universal impedance fluctuations

described by the Random Matrix Theory (RMT).[11–13] According to the theory, for a two port system[47,48]

$$\xi_{rmt,a,b} = \sum_{m=1}^{M} \frac{W_{am} W_{bm}}{\lambda_m^{rmt} - i\alpha}. \tag{3}$$

The element $\xi_{rmt,a,b}$ is the impedance between port a and port b, and the sum is over the M eigenmodes of the closed wave scattering enclosure, W_{am} (or W_{bm}) represents the coupling between the port a (or the port b) and the mth eigenmode. Based on the assumption of the random plane wave hypothesis (the Berry hypothesis), for a wave-chaotic cavity enclosure filled with reciprocal media (i.e., that has time-reversal invariance), W_{am} and W_{bm} are independent Gaussian random variables of zero mean and unit variance.[47] λ_m^{rmt} is the mth eigenvalue of a large random matrix. The statistics of these eigenvalues are based on RMT, and they are found from a large random matrix selected from the GOE (Gaussian Orthogonal Ensemble) for the time-reversal-invariant case. The details of generating λ_m^{rmt} are discussed in Appendix A of Ref. 50. The loss parameter α is the only parameter determining the statistics of the universal fluctuations. In the case of a two-dimensional billiard the loss parameter is given by $\alpha = k^2 A/(4\pi Q)$ and can be interpreted as the ratio of the typical 3-dB bandwidth of the resonant modes to the mean spacing in frequency between the modes. $k = 2\pi f/c$ is the wave number of frequency f, A represents the area of the billiard, and Q is the typical loaded quality factor of the enclosure under the assumption that losses are uniform.

The algorithm for generating $\overline{\overline{\xi}}_{rmt}$ can be developed based on Eq. (3). By varying α, the universal statistics of $\overline{\overline{\xi}}$ for systems with varying losses can be numerically generated, and examples of these distributions are given in Ref. 49. Starting with a statistical ensemble data set and going the other way around, one can fit the experimentally extracted $\overline{\overline{\xi}}$ to $\overline{\overline{\xi}}_{rmt}(\alpha)$, and the best matching distributions will give an estimate of the loss parameter of the experimental system. Note that when examining data, for a two port system, $\overline{\overline{\xi}}$ can produce 8 histograms, i.e., real and imaginary part for each element $\xi_{a,b}$. However due to the reciprocity of the system, $\xi_{12} = \xi_{21}$, and ξ_{11} has the same statistics as ξ_{22} according to Eq. (3). As a result there are 4 unique histograms that are simultaneously fit using a single loss parameter α. Experimental tests in various wave chaotic systems have systematically explored the effects of different loss parameters on the statistical properties of impedance, ranging from cryogenic superconducting cavities ($\alpha \sim 0.01$)[50,51] to three-dimensional complex enclosures ($\alpha > 10$).[27]

Here, a symmetry-reduced "1/4-bowtie" shape (Fig. 1) quasi-two-dimensional cavity at room temperature is used as the ray chaotic system.[6] To introduce nonlinearity, an active nonlinear circuit is connected to two ports of the billiard as shown in Fig. 1. The active nonlinear circuit is designed to double the input frequency in the range from 3.5 GHz to 4.5 GHz; other harmonics, as well as the fundamental tone, are suppressed at the output. Measurements are taken between two additional ports of the cavity, and an ensemble of billiard realizations is created by moving two perturbers throughout the cavity. Thus, the realizations maintain a fixed volume and mean mode spacing. A sinusoidal tone at fundamental frequency 1f with a certain power is created in the Vector Network Analyzer (VNA) and injected through port 1. Port 3 is the input of the active nonlinear circuit. Due to the ray-chaotic properties of the cavity, the 1f signal received by port 3 varies over several decades in power as a function of frequency and perturber locations. The output at port 4 will be at the 2nd harmonic frequency with a certain power. Port 4 serves as the source of a 2f signal injected into the cavity. The VNA is set in the Frequency Offset Mode (FOM), which provides the capability to have the VNA sources apply a tone at one frequency and the receivers measure the response at any other frequency. In our case, the VNA port 2 measures the absolute power of the 2nd harmonics of the stimulus from port 1.

III. MODEL

We separately characterize the nonlinear circuit under FOM and find that for input powers in the range −45 dBm to −5 dBm, $P_{out,2f}$ *vs.* $P_{in,1f}$ obeys a simple empirical relation:

$$P_{out,2f} = slope \cdot P_{in,1f} + intercept \qquad (\text{dBm}), \tag{4}$$

where $slope = 2.00 \pm 0.01$ and the amplifier contributes to the "intercept" term. Note that power P is in dBm and the "intercept" here refers to intercept in units of dBm, i.e., $P_{out,2f}$ when $P_{in,1f} = 0$ dBm. In terms of power measured in Watts, since $P_{dBm} = 10\log(10^3 \times P_W)$, Eq. (4) is effectively $P_{out,2f} = P_{in,1f}^2 \cdot P_{norm}$, where $P_{norm} = 10^6 \times P_{intercept}$, and $P_{intercept}$ is *intercept* converted into units of Watts.

To describe the statistical properties of the second harmonic signals measured at port 2, a model of two cascaded linear cavities connected through the nonlinear circuit is proposed (see Fig. 2). This choice was motivated by earlier work on the statistics of impedance and power fluctuations in chains of wave chaotic cavities connected by weak but linear coupling.[29,30,45] As shown in Fig. 2, the source signal enters the cavity from port 1. The signal reaching port 3, which is the input of the nonlinear circuit, is given by the linear transmission S-parameters between port 1 and 3, denoted by S_{13}. Its statistics are described by the linear Random Coupling Model at 1f with loss parameter α_1. The output signals of the nonlinear circuit at port 4 are at the 2nd harmonic of the input at port 3. Their relation is characterized by the empirical law of the active nonlinear circuit, Eq. (4). Lastly, the 2nd harmonic signals received at port 2 are linearly related to the 2nd harmonic signals introduced at port 4, which is given by the statistical fluctuations of the transmission S-parameters between port 2 and port 4 denoted by S_{24}. The statistics of S_{24} are described by the linear Random Coupling Model at frequency 2f with loss parameter α_2. Since the vector network analyzer in FOM measures power, we have a simple relation for the power of 2nd harmonics received at port 2,

$$P_{out,2f} = (P_{in,1f} \cdot |S_{13}|^2)^2 \cdot P_{norm} \cdot |S_{24}|^2 \qquad (\text{Watts}), \tag{5}$$

where $P_{in,1f}$, P_{norm} are deterministic, in units of Watts; and $|S_{13}|^2$, $|S_{24}|^2$ are fluctuating quantities.

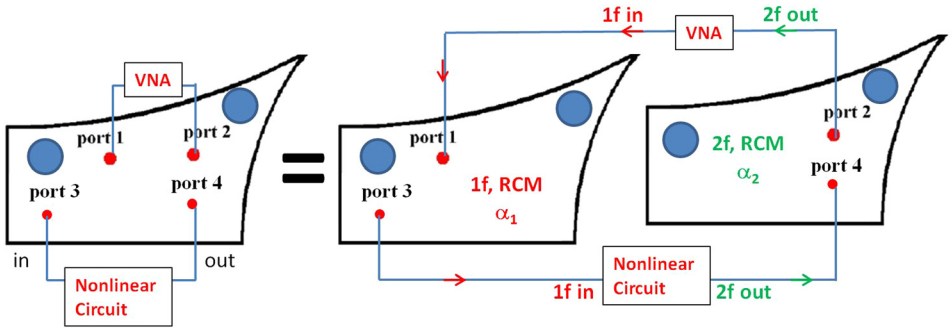

FIG. 2. Model of the nonlinear billiard in terms of cascaded cavities. The bowtie with an active nonlinear circuit attached can be considered as two linear billiards operating at different frequencies and loss parameters coupled through the nonlinear circuit.

IV. RESULTS

In the results shown below, there are 136 realizations for $P_{in,1f} = -5$ dBm input, 99 for 0 dBm, and 91 for +5 dBm, respectively. For each realization, the VNA outputs a $1f$ signal sweeping from 3.5 GHz to 4.5 GHz with fixed power at port 1, which is $P_{in,1f}$. With the FOM one then measures the response 2nd harmonics at port 2, $P_{out,2f}$. For each $1f$ input power, the histograms of power values of $P_{out,2f}$ are compiled over the ensemble of realizations as well as the second harmonic frequency between 7 and 9 GHz. These histograms of the measured 2nd harmonic power are plotted in Fig. 3 and will be compared with theory predictions.

To test the extended RCM model, we have two approaches. The "measured product" is a calculation based on separate measurement of each linear component, i.e., measurements of S_{13}, S_{24}. S-parameters between ports 1 and 3 are measured at 3.5–4.5 GHz, for 120 realizations of the positions of the perturbers. The S-parameters between ports 2 and 4 are measured at 7–9 GHz, again for 120 different realizations of the perturber positions. In the direct experimental measurement of the $2f$ signal with the $1f$ input, the $1f$ and $2f$ signals pass through the cavity with the same perturber position. However, in the "measured product," the S-parameters S_{13} and S_{24} are measured independently, each with a separate ensemble of perturber positions. Their values will not correspond directly to those in the case in which the entire transfer function is characterized. Statistically, the histograms for the "measured product" and "experiment" will correspond if S_{13} and S_{24} are effectively independent. By putting the measured quantities into the relation Eq. (5), we create 120^2 "realizations" of $P_{out,2f}$. We call this a "super data set" and its P_{2f} statistics can be compared with those measured directly.

Another approach, termed "simulation," utilizes the RCM to generate a prediction for the statistical distribution of power values. By using the measured ensembles of $\overline{\overline{S}}_{13}(1f)$ mentioned above, $\overline{\overline{Z}}_{avg,13}(1f)$ can be derived by averaging over realizations. The RCM formulation [Eq. (2)] is applied to extract $\overline{\overline{\xi}}(1f)$ from the ensemble data. By fitting the histograms of $\overline{\overline{\xi}}(1f)$, the loss parameter α_1 between 3.5 GHz and 4.5 GHz is estimated. In practice, for each frequency window of 0.5 GHz, the loss parameter α_1 is determined as the average loss parameter obtained from fitting the histograms of the off-diagonal impedance elements $Re\{\overline{\overline{\xi}}_{12}(1f)\}$ and $Im\{\overline{\overline{\xi}}_{12}(1f)\}$. The same procedures are applied to the measured ensembles of $\overline{\overline{S}}_{24}(2f)$ to derive $\overline{\overline{Z}}_{avg,24}(2f)$ and α_2 between 7 and 9 GHz. Having the $\overline{\overline{Z}}_{avg}$ and loss parameters in the two frequency ranges of interest, we can perform Monte Carlo RMT simulations based on Eq. (3) to firstly get normalized impedance $\overline{\overline{\xi}}$, then to generate ensembles of S_{13} and S_{24} using RCM [Eqs. (2) and (1)]. This approach can be considered as a validity test of the RCM. Again, we generate 120 realizations of S_{13} and S_{24} respectively, and substitute them into Eq. (5) to create a "super

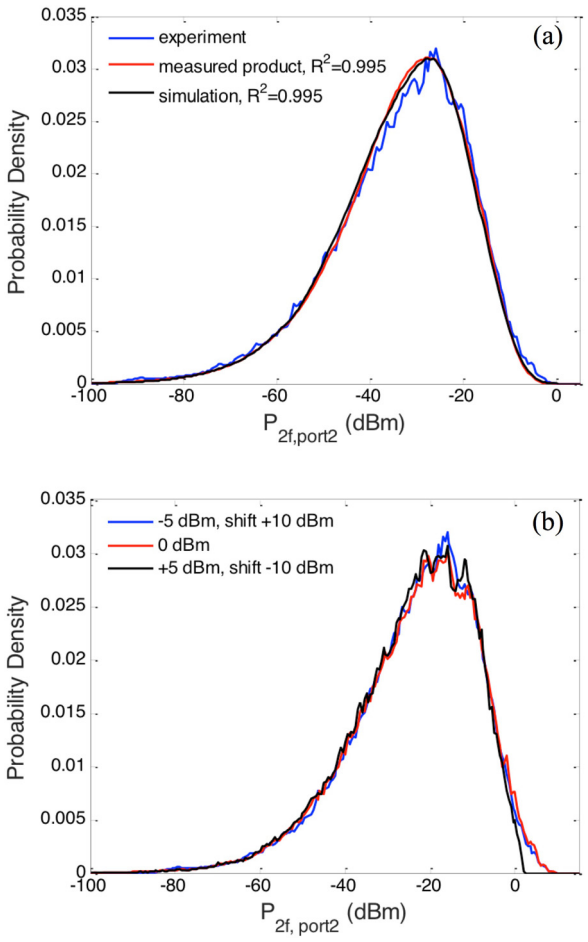

FIG. 3. Measurement of second harmonic power statistics and test of the model of cascaded cavities. (a) The statistics of the output 2nd harmonic power predicted by the model are compared with the direct measurement results (blue). The statistics are compiled over a 2 GHz range with a center frequency of 8 GHz. (b) Three input powers are measured: −5 dBm, 0 dBm, and +5 dBm, and the distributions are shifted by ±10 dBm (±10 dBm) to overlap. The cutoff near 0 dBm for the +5 dBm curve comes from the saturation of the VNA (Model E8364C). For $P_{in,1f} = -5$ dBm, 0 and 5 dBm, the mean value is −33.6 dBm, −23.6 dBm and −14.3 dBm, respectively. The standard deviations are 14.6 dBm, 14.8 dBm, and 14.4 dBm, respectively.

data set" prediction for the histogram of $P_{out,2f}$. The result is based on simulated universal quantities "dressed" by the measured non-universal features.

The loss parameters α at $1f$ and $2f$ are both less than 1. In such a low loss chaotic environment, the individual cavity mode contributions to the S-parameters will be sharp and distinct. The value of $P_{in,1f}$ at port 1 is set so that the majority $1f$ power at port 3 falls within the range where Eq. (4) holds. As a result, the power of the second harmonic signal spans a wide range. Figure 3 shows histograms of the second harmonic power plotted on a log scale with units of dBm. The histogram is compiled from an ensemble of realizations and over a $2f$ output frequency range from 7 to 9 GHz. For a fixed input power over a certain frequency band, the 2nd harmonic output power varies over 8 – 10 decades. For example, Fig. 3(a) shows the result for input power $P_{in,1f} = -5$ dBm. The blue curve is the histogram from direct measurement, where the received power of the 2nd harmonics varies from -100 dBm to 0 dBm. It has a mean of -14.3 dBm and a standard deviation of 14.4 dBm. The red curve is the "measured product," also derived from measurement. Although derived by a different approach, the overall statistics agrees very well with our direct measurement of the second harmonic power. The black curve labeled "simulation" is created based on the RCM as described above, and as shown in the plots, it agrees quite well with the red and blue curves, demonstrating the validity of the Random Coupling Model.

To quantify the agreement, the coefficient of determination R^2 traditionally used in statistics is calculated for each model histogram with respect to the experimental curve. R^2 is always between 0 and 1 and is interpreted as the percentage of variation in the response variable that is explained by the linear model.[52] In general, the higher the R^2, the better the model fits to the data. The red curve "measured product" has $R^2 = 0.995$ and the black curve "simulation" has $R^2 = 0.994$, both indicating very good agreement. We emphasize that this model yielding this agreement has *no fitting parameter*.

The model [Eq. (5)] predicts that changing the input power should simply shift the PDFs of $P_{out,2f}$ by 10 dB for each 5 dB increase in input power. Figure 3(b) shows the shifted curves of the experimental results with respect to the 0 dBm case. Indeed the overall distribution has a similar shape for each input power. However, experimentally the VNA reaches its maximum detectable power at nearly 15 dBm. This is why there is a cutoff at high power for the curve of $P_{in,1f} = 5$ dBm. The results of RCM-based model fits to the second harmonic statistics for input power $P_{in,1f} = 0$ and 5 dBm are shown in the supplementary material.

V. FURTHER ANALYSIS AND DISCUSSION

Prior work[44] has investigated second harmonic generation by nonlinear electronics irradiated in a reverberation chamber (RC). This situation involves a "bare" nonlinear source without filtering or amplification, producing a small nonlinear response with a low signal-to-noise ratio. The statistics of the re-radiated harmonic spectrum were investigated by using a model of cascaded random processes. Under the assumption that the distribution of the linear field statistics in the reverberation chamber follow a Rayleigh distribution, a combined Rayleigh distribution was derived for the statistics of the harmonics.[44] However, it has been shown that the Rayleigh distribution of the field statistics in a cavity is only valid in the high-loss regime (loss parameter $\alpha \gg 1$).[53,54] By introducing microwave absorbers into the perimeter of the billiards[26,55] or putting the billiard in a dry ice low temperature environment, we are able to tune the loss parameter α from 0.1 to 6 or higher. We show in the supplementary material that the Rayleigh model for linear S-parameter statistics fails in the low loss environment, although the RCM is still valid (supplementary material). As a result, the RCM-based model shows much better agreement with the 2nd harmonic field statistics than the combined Rayleigh model. Further, a more versatile "Double Weibull" model was developed that takes into account the saturation of the nonlinear element.[56,57] The fitting parameter in this model is directly related to the nonlinear exponent [*slope* in Eq. (4)]. The combined Rayleigh distribution is a special case of a "Double Weibull" model with $n = 2$, and the "Double Weibull" model assumes that $n < 2$ as the nonlinear element saturates. Our results show that the fitting parameter changes dramatically with loss in the billiard (for a fixed nonlinear transfer function *slope* $= 2$), and that the values are un-physical in the low loss case. The detailed results are given in the supplementary material. In the engineering context, testing a bare nonlinear element in an RC has applications for EMC (electromagnetic compatibility) immunity testing. Those models work well in RC settings where the loss parameter $\alpha \gg 1$, but have not been tested in a low-loss setting such as those in our experiments. The RCM-based model holds in both high loss and low loss cases, without any fitting parameters, and thus we conclude that the RCM-based model is a more accurate and physically realistic description of the system.

VI. CONCLUSIONS

In summary, by adding an active nonlinear circuit to the ray-chaotic 1/4-bowtie cavity, and extending the Random Coupling Model, it is possible to predict the statistics of harmonics in a nonlinear wave chaotic system. The model of nonlinear cascaded cavities Eq. (5), which incorporates nonlinearity into the Random Coupling Model, describes the effects of the active nonlinear circuit, and is valid both in the low loss and high loss regimes. This is the first effort to extend the RCM to the nonlinear domain. It is shown to be more general compared to previous models of similar phenomena. The model does not require any fitting parameters although a fair amount of independently-determined system-specific information is incorporated into the model. The artificially fabricated nonlinear circuit is uni-directional, filtered, and amplified to produce only 2nd harmonics, making the system simple to analyze. It paves the way for generalizing RCM to more complicated nonlinear situations. It also offers

an approach to nonlinear problems in acoustic, optical, atomic, and other chaotic systems.

SUPPLEMENTARY MATERIAL

See the supplementary material for: (I) results of the extended RCM model [Eq. (5)] fits to second harmonic power statistics of input power $P_{in,1f} = 0$ dBm and $+5$ dBm, respectively. (II) Results of comparison with other models (Rayleigh model to linear fields, Combined Rayleigh, and Double Weibull model to second harmonic fields).

ACKNOWLEDGMENTS

This work is supported by the ONR under Grant No. N000141512134, the AFOSR under COE Grant No. FA9550-15-1-0171, the COST Action IC1407 "ACCREDIT" supported by COST (the European Cooperation in Science and Technology), and the Maryland Center for Nanophysics and Advanced Materials (CNAM).

[1]Y. Alhassid, "The statistical theory of quantum dots," Rev. Mod. Phys. **72**, 895 (2000).
[2]P. W. Brouwer and C. W. J. Beenakker, "Voltage-probe and imaginary-potential models for dephasing in a chaotic quantum dot," Phys. Rev. B **55**, 4695 (1997).
[3]R. U. Haq, A. Pandey, and O. Bohigas, "Fluctuation properties of nuclear energy levels: Do theory and experiment agree?," Phys. Rev. Lett. **48**, 1086 (1982).
[4]R. G. Newton, *Scattering Theory of Waves and Particles* (McGraw-Hill, New York, 1966).
[5]E. Doron, U. Smilansky, and A. Frenkel, "Experimental demonstration of chaotic scattering of microwaves," Phys. Rev. Lett. **65**, 3072 (1990).
[6]P. So, S. M. Anlage, E. Ott, and R. N. Oerter, "Wave chaos experiments with and without time reversal symmetry: GUE and GOE statistics," Phys. Rev. Lett. **74**, 2662 (1995).
[7]U. Kuhl, M. Martínez-Mares, R. A. Méndez-Sánchez, and H.-J. Stöckmann, "Direct processes in chaotic microwave cavities in the presence of absorption," Phys. Rev. Lett. **94**, 144101 (2005).
[8]R. L. Weaver, "Spectral statistics in elastodynamics," J. Acoust. Soc. Am. **85**, 1005 (1989).
[9]C. Ellegaard, T. Guhr, K. Lindemann, H. Q. Lorensen, J. Nygård, and M. Oxborrow, "Spectral statistics of acoustic resonances in aluminum blocks," Phys. Rev. Lett. **75**, 1546 (1995).
[10]B. T. Taddese, G. Gradoni, F. Moglie, T. M. Antonsen, E. Ott, and S. Mark Anlage, "Quantifying volume changing perturbations in a wave chaotic system," New J. Phys. **15**, 023025 (2013).
[11]G. Casati, F. Valz-Gris, and I. Guarneri, "On the connection between quantization of nonintegrable systems and statistical theory of spectra," Lett. Nuovo Cimento **28**, 279 (1980).
[12]O. Bohigas, M. J. Giannoni, and C. Schmit, "Characterization of chaotic quantum spectra and universality of level fluctuation laws," Phys. Rev. Lett. **52**, 1–4 (1984).
[13]H. J. Stöckmann, *Quantum Chaos: An Introduction* (Cambridge University Press, Cambridge, 1999).
[14]S. Hemmady, X. Zheng, T. M. Antonsen, E. Ott, and S. M. Anlage, "Universal statistics of the scattering coefficient of chaotic microwave cavities," Phys. Rev. E **71**, 056215 (2005).
[15]*The Oxford Handbook of Random Matrix Theory*, edited by G. Akemann, J. Baik, and P. Di Francesco (Oxford University Press, Oxford, 2010).
[16]Y. V. Fyodorov, D. V. Savin, and H.-J. Sommers, "Scattering, reflection and impedance of waves in chaotic and disordered systems with absorption," J. Phys. A **38**, 10731 (2005).
[17]B. Dietz and A. Richter, "Quantum and wave dynamical chaos in superconducting microwave billiards," Chaos **25**, 097601 (2015).
[18]D. H. Wu, J. S. A. Bridgewater, A. Gokirmak, and S. M. Anlage, "Probability amplitude fluctuations in experimental wave chaotic eigenmodes with and without time-reversal symmetry," Phys. Rev. Lett. **81**, 2890 (1998).
[19]S.-H. Chung, A. Gokirmak, D.-H. Wu, J. S. A. Bridgewater, E. Ott, T. M. Antonsen, and S. M. Anlage, "Measurement of wave chaotic eigenfunctions in the time-reversal symmetry-breaking crossover regime," Phys. Rev. Lett. **85**, 2482 (2000).
[20]X. Zheng, S. Hemmady, T. M. Antonsen, Jr., S. M. Anlage, and E. Ott, "Characterization of fluctuations of impedance and scattering matrices in wave chaotic scattering," Phys. Rev. E **73**, 046208 (2006).
[21]J. A. Hart, T. M. Antonsen, and E. Ott, "The effect of short ray trajectories on the scattering statistics of wave chaotic systems," Phys. Rev. E **80**, 041109 (2009).
[22]J.-H. Yeh, J. Hart, E. Bradshaw, T. Antonsen, E. Ott, and S. M. Anlage, "Universal and non-universal properties of wave chaotic scattering systems," Phys. Rev. E **81**, 025201(R) (2010).
[23]J.-H. Yeh, J. Hart, E. Bradshaw, T. Antonsen, E. Ott, and S. M. Anlage, "Experimental examination of the effect of short ray trajectories in two-port wave-chaotic scattering systems," Phys. Rev. E **82**, 041114 (2010).
[24]F. Beck, C. Dembowski, A. Heine, and A. Richter, "R-matrix theory of driven electromagnetic cavities," Phys. Rev. E **67**, 066208 (2003).
[25]O. Hul, S. Bauch, P. Pakonski, N. Savytskyy, K. Zyczkowski, and L. Sirko, "Experimental simulation of quantum graphs by microwave networks," Phys. Rev. E **69**, 056205 (2004).
[26]S. Hemmady, X. Zheng, E. Ott, T. M. Antonsen, and S. M. Anlage, "Universal impedance fluctuations in wave chaotic systems," Phys. Rev. Lett. **94**, 014102 (2005).
[27]Z. B. Drikas, J. G. Gil, H. V. Tran, S. K. Hong, T. D. Andreadis, J.-H. Yeh, B. T. Taddese, and S. M. Anlage, "Application of the random coupling model to electromagnetic statistics in complex enclosures," IEEE Trans. Electromagn. Compat. **56**, 1480–1487 (2014).
[28]M.-J. Lee, T. M. Antonsen, and E. Ott, "Statistical model of short wavelength transport through cavities with coexisting chaotic and regular ray trajectories," Phys. Rev. E **87**, 062906 (2013).
[29]G. Gradoni, J.-H. Yeh, T. M. Antonsen, S. M. Anlage, and E. Ott, "Wave chaotic analysis of weakly coupled reverberation chambers," in *Proceedings of the 2011 IEEE International Symposium on Electromagnetic Compatibility* (2011), pp. 202–207.
[30]G. Gradoni, T. M. Antonsen, and E. Ott, "Impedance and power fluctuations in linear chains of coupled wave chaotic cavities," Phys. Rev. E **86**, 046204 (2012).
[31]E. J. Heller, L. Kaplan, and A. Dahlen, "Refraction of a Guassian seaway," J. Geophys. Res. **113**, C09023 (2008).
[32]R. Höhmann, U. Kuhl, H.-J. Stöckmann, L. Kaplan, and E. J. Heller, "Freak waves in the linear regime: A microwave study," Phys. Rev. Lett. **104**, 093901 (2010).
[33]K. Dysthe, H. E. Krogstad, and P. Müller, "Oceanic rogue waves," Annu. Rev. Fluid Mech. **40**, 287–310 (2008).
[34]M. Onorato, S. Residori, U. Bortolozzo, A. Montina, and F. T. Arecchi, "Rogue waves and their generating mechanisms in different physical contexts," Phys. Rep. **528**, 47 (2013).
[35]B. Van Damme, K. Van Den Abeele, Y. F. Li, and O. B. Matar, "Time reversed acoustics techniques for elastic imaging in reverberant and nonreverberant media: An experimental study of the chaotic cavity transducer concept," J. Appl. Phys. **109**(10), 104910 (2011).
[36]R. Guyer and P. Johnson, "Nonlinear mesoscopic elasticity: Evidence for a new class of materials," Phys. Today **52**(4), 30 (1999).
[37]K. E. A. Van Den Abeele, A. Sutin, J. Carmeliet, and P. A. Johnson, "Micro-damage diagnostics using nonlinear elastic wave spectroscopy (NEWS)," NDT&E Int. **34**(4), 239–248 (2001).
[38]G. Lerosey, J. de Rosny, A. Tourin, and M. Fink, "Focusing beyond the diffraction limit with far-field time reversal," Science **315**, 1120 (2007).
[39]M. Frazier, B. Taddese, T. Antonsen, and S. M. Anlage, "Nonlinear time-reversal in a wave chaotic system," Phys. Rev. Lett. **110**, 063902 (2013).
[40]M. Frazier, B. Taddese, B. Xiao, T. Antonsen, E. Ott, and S. M. Anlage, "Nonlinear time reversal of classical waves: Experiment and model," Phys. Rev. E **88**, 062910 (2013).
[41]S. Gnutzmann, U. Smilansky, and S. Derevyanko, "Stationary scattering from a nonlinear network," Phys. Rev. A **83**, 033831 (2011).
[42]S. D. Cohen, H. L. D. S. Cavalcante, and D. J. Gauthier, "Subwavelength position sensing using nonlinear feedback and wave chaos," Phys. Rev. Lett. **107**, 254103 (2011).
[43]L. Guibert, P. Millot, X. Ferrieres, and E. Sicard, "An original method for the measurement of the radiated susceptibility of an electronic system using induced electromagnetic nonlinear effects," Prog. Electromagn. Res. Lett. **62**, 83–89 (2016).

[44]I. Flintoft, A. Marvin, and L. Dawson, "Statistical response of nonlinear equipment in a reverberation chamber," in *2008 IEEE International Symposium on Electromagnetic Compatibility* (Detroit, MI, 2008), pp. 1–6; available at http://ieeexplore.ieee.org/document/4652024/.
[45]G. Gradoni, J.-H. Yeh, B. Xiao, T. M. Antonsen, S. M. Anlage, and E. Ott, "Predicting the statistics of wave transport through chaotic cavities by the random coupling model: A review and recent progress," Wave Motion **51**, 606–621 (2014).
[46]S. Hemmady, X. Zheng, T. M. Antonsen, E. Ott, and S. M. Anlage, "Universal properties of 2-port scattering, impedance and admittance matrices of wave chaotic systems," Phys. Rev. E **74**, 036213 (2006).
[47]X. Zheng, T. M. Antonsen, and E. Ott, "Statistics of impedance and scattering matrices in chaotic microwave cavities: Single channel case," Electromagnetics **26**, 3–35 (2006).
[48]X. Zheng, T. M. Antonsen, Jr., and E. Ott, "Statistics of impedance and scattering matrices of chaotic microwave cavities with multiple ports," Electromagnetics **26**, 37 (2006).
[49]S. Hemmady, T. M. Antonsen, Jr., E. Ott, and S. M. Anlage, "Statistical prediction and measurement of induced voltages on components within complicated enclosures: A wave-chaotic approach," IEEE Trans. Electromagn. Compat. **54**, 758–771 (2012).
[50]J.-H. Yeh and S. Analge, "In-situ broadband cryogenic calibration for two-port superconducting microwave resonators," Rev. Sci. Instrum. **84**, 034706 (2013).
[51]J.-H. Yeh, Z. Drikas, J. G. Gil, S. Hong, B. T. Taddese, E. Ott, T. M. Antonsen, T. Andreadis, and S. M. Anlage, "Impedance and scattering variance ratios of complicated wave scattering systems in the low loss regime," Acta Phys. Pol., A **124**, 1045 (2013).
[52]M. Lefebvre, *Applied Probability and Statistics* (Springer, New York, 2006).
[53]J.-H. Yeh, E. Ott, T. M. Antonsen, and S. M. Anlage, "Fading statistics in communications—A random matrix approach," Acta Phys. Pol., A **120**, A-85 (2011).
[54]J.-H. Yeh, T. M. Antonsen, E. Ott, and S. M. Anlage, "First-principles model of time-dependent variations in transmission through a fluctuating scattering environment," Phys. Rev. E (Rapid Communications) **85**, 015202 (2012).
[55]S. Hemmady, J. Hart, X. Zheng, T. M. Antonsen, Jr., E. Ott, and S. M. Anlage, "Experimental test of universal conductance fluctuations by means of wave-chaotic microwave cavities," Phys. Rev. B **74**, 195326 (2006).
[56]A. C. Marvin, C. Jiaqi, I. D. Flintoft, and J. F. Dawson, "A describing function method for evaluating the statistics of the harmonics scattered from a non-linear device in a mode stirred chamber," in *2009 IEEE International Symposium on Electromagnetic Compatibility*, *Austin, TX* (2009), pp. 165–170; available at http://ieeexplore.ieee.org/document/5284689/.
[57]C. Jiaqi, A. Marvin, I. Flintoft, and J. Dawson, "Double-Weibull distributions of the re-emission spectra from a non-linear device in a mode stirred chamber," in *2010 IEEE International Symposium on Electromagnetic Compatibility*, *Fort Lauderdale, FL* (2010), pp. 541–546; available at http://ieeexplore.ieee.org/document/5711334/.